Novel Monolithic Stirred Reactor

Rolf K. Edvinsson Albers, Marco J. J. Houterman, Theo Vergunst, Eric Grolman, and Jacob A. Moulijn
Dept. of Chemical Engineering, Delft University of Technology, Julianalaan 136, 2628 BL Delft, The Netherlands

A novel reactor configuration in which blocks of monoliths are arranged in a stirrer-like configuration was studied. A substantial liquid flow rate can be realized through the monolith blades at relatively low power input, owing to the high permeability of the monolithic structure. The inside of the monolithic channels can be coated with a thin layer of either a conventional catalyst or a biocatalyst, thereby eliminating many of the problems associated with using a suspended catalyst. The basic relationship among stirrer speed, geometry, liquid viscosity, and the resulting torque and flow through the blades were studied. Furthermore, the fast decomposition of a dilute, aqueous hydrogen peroxide solution was used to characterize the rate of external mass transfer.

Introduction

It is often necessary to bring a liquid-phase reactant into contact with a solid catalyst. Immobilized bioactive materials like cells or enzymes can also be regarded as examples of solid catalysts. The catalyst can often be applied in the form of a fine powder suspended in the liquid in order to maximize the contact area and minimize the intraparticle diffusion distances. There are, however, several potential problems associated with the handling of powdered catalysts: separation, attrition, erosion of the equipment, and the hazards of handling in the case of pyrophoric catalysts. The complex hydrodynamics of slurries makes scale-up difficult, which can lead to problems like incomplete suspension of particles and nonuniform distribution of catalyst.

One solution is to fix the catalyst to a stirrer. For catalytic gas-phase reactions this has been done with a catalyst-filled basket (Carberry, 1964) and with a monolithic catalyst (Bennet et al., 1991), both spinning at high speed.

Turek and Winter (1990) used a spinning basket reactor to study catalytic gas–liquid reactions but failed to obtain sufficient flow rates through the catalyst packing because of its high resistance to flow.

A possible solution is to use a highly permeable packing. Figure 1 shows the permeability coefficient as a function of the geometrical surface area for both a packed bed of spherical particles as estimated by Kozeny's equation (Coulson and Richardson, 1985) and a monolith with cells of square cross section assuming fully developed laminar flow. It follows that for identical geometrical surface area, the resistance to flow is about one order of magnitude lower for the monolith. This fact is the main reason behind the monolith's widespread use in emission control.

Kolaczkowski and Serbetcioglu (1994) studied the preparation of siloxane polymers using a monolithic catalyst. They used a fixed-bed configuration and a configuration with the monolith mounted on a stirrer shaft. The performance of the latter was poor, probably because of the high viscosity of the polymer solution.

In this work we will show that a monolithic stirrer does work for a low-viscosity liquid (water). Torque and stirrer speed were measured experimentally and a simple model for predicting the flow rate through the monolith structure was developed. The following fast first-order decomposition reaction of a dilute, aqueous hydrogen peroxide solution on a manganese oxide catalyst was used to characterize mass transfer:

$$H_2O_2(aq) \Rightarrow H_2O(l) + \frac{1}{2}O_2(g); \qquad r = k_0 e^{-\frac{E_a}{RT}} c \quad (1)$$

This method has previously been used to characterize a trickle-bed reactor (Wu et al., 1996) and a monolith reactor operating in single- and two-phase flow (Vergunst et al., 1997).

Correspondence concerning this article should be addressed to J. A. Moulijn.
Current address of R. K. E. Albers: Bleaching Chemicals Div., Eka Chemicals AB, SE-445 80 Bohus, Sweden.
Current address of M. J. J. Houterman: Shell Chemicals, P.O. Box 6060, 4780 LN Moerdijk, The Netherlands.
Current address of E. Grolman: DSM Research, P.O. Box 18, 6160 MD Geleen, The Netherlands.

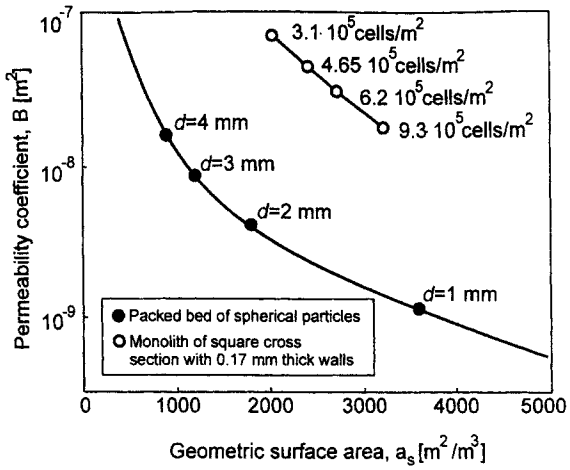

Figure 1. Permeability coefficient as a function of the external surface area.

For a bed consisting of spherical particles and for a monolith of square cross section with 0.17-mm-thick walls.

Experimental Studies

Monolithic stirrer setup

The setup and main dimensions are shown in Figure 2. The Perspex tank used is equipped with six baffles attached to the wall with a small clearance. The stirrer is driven by a DC motor (Portescap Escap 22V28-216E, 4.2W) equipped with a reduction gearbox (Escap K24, 32:1) via a flexible coupling. The DC motor is connected to a controller that also acts as the power supply. The shaft speed and torque can be calculated from the measured current and voltage. The stirrer speed was measured by counting the pulses generated when a disk with a large number of slits intersected a light beam. This principle is also used in computers for pointing devices. A modified computer mouse (Logitech Mouse M-M30) was used.

The concentration of hydrogen peroxide was measured on-line amperometrically using a platinum dual-electrode system (ProMinent GmbH, Dulcometer PEROX 21, range 200–2,000 ppm). The PEROX 21 is also equipped with pH and temperature sensors. The whole setup was connected to a PC for data logging and control.

The monoliths used in the hydrodynamics study were uncoated cordierite monoliths of square cross-section (Corning Inc., Corning, N.Y.). The wall thickness was 170 μm and the cell density was 62 cells/cm^2 (400 cpsi). Three types of experiments were performed:

(1) *Open monolith*, the normal mode of operation.

(2) *Closed monolith*, whereby the front area of the monolith was covered by a thin plastic film.

(3) *Empty tube*, whereby the monolith was replaced by an empty pipe of the same external dimensions.

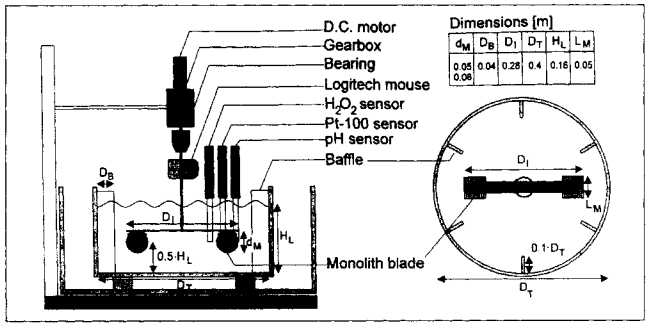

Figure 2. Monolithic catalyst stirrer reactor setup.

Catalyst preparation

Monoliths washcoated with an ~ 30-μm-thick layer of alumina (100 g/L, Degussa AG, Hanau, Germany) were used to prepare the manganese oxide catalyst following the method of Kapteijn et al. (1994). The monolith was impregnated using a 1.6-M manganese acetate tetrahydrate (Fluka, > 99% p.a.) solution for 2 h (room temperature). After blowing excess solution from the channels it was dried in a microwave oven (Whirlpool ProMicro 825) at 550 W for 15 min. The fast and uniform heating resulting from the use of a microwave oven ensures a homogeneous distribution of catalyst. Subsequently the monolith was calcined in air (5 K/min to 723 K and kept there for 2 h). The procedure was repeated once to give a total manganese oxide load of 5 wt. %. By cutting one of the samples it was found that all channels had obtained the brown color, characteristic of a uniformly distributed manganese oxide.

Deionized water was used for the hydrodynamics study. In the reaction runs a starting solution containing 1,500 ppm H_2O_2 (Merck, 30 wt. %, p.a.) and 0.01-M $Na_2SO_4 \cdot 10\ H_2O$ (Merck, > 99 wt. %, p.a.) was applied. The sodium sulfate was added to ensure that the minimum conductivity of 100 μS/cm required for the amperometric hydrogen peroxide measurement was obtained. The measurement was insensitive to concentration of sodium sulfate.

The molecular diffusivity of hydrogen peroxide was estimated to $2.3 \cdot 10^{-9}$ m^2/s using the method of Wilke and Chang (1955).

A detailed description of the experimental procedure is given by Houterman (1997).

Theory

Flow inside the monolith channels

The mean flow velocity in a channel of square cross-section can be approximated by Eq. 2. The values for long channels are taken from Perry (1984). The dependency on length is assumed to be the same as for cylindrical channels, which is given by Shah and London (1971).

$$u = \frac{\Delta P d_h^2}{28.46 \mu L}\left(1 + 0.0445\ Re \frac{d_h}{L}\right)^{-0.5} \qquad (2)$$

In our case the correction factor for entrance effects is always close to one. Since entrance effects can be neglected Eq. 2 can be cast in the same form as Darcy's law:

$$u_{sup} = \frac{B}{\mu}\frac{\Delta P}{L}$$

where

$$B = \frac{A_{\text{open}} d_h}{28.46} \tag{3}$$

Flow through the monolith blade

We assume that the dimensions of the monolith blade are small compared to the diameter of the impeller, the velocity of the monolith relative to the surrounding liquid does not vary with time, the liquid swirl is negligible (supported by observation of neutrally buoyant particles), and the blades are far away from the vessel walls. Some of these assumptions are not fully realistic. However, they represent an idealized situation in which a piece of a monolith is moved through a fluid. This model is useful for establishing the fundamental relationships and serves as a starting point for more refined models.

The relative motion between the monolith blade and the surrounding liquid causes a pressure difference to build up across the blade, which is approximately proportional to ρU^2 for an impermeable blade, where U is the tip velocity of the blade. If the blade is permeable a fraction of the liquid will pass through the blade and the pressure difference across the blade will be lower. The flow through the blade gives rise to a frictional pressure drop proportional to $\alpha UL\mu/B$ (from Eq. 3), where α is the fraction of the liquid swept that passes through the blade. Setting these two pressure differences equal to each other in the case when α is close to zero (essentially impermeable blade) leads to

$$\alpha \propto \frac{\left(\frac{B}{L}\right)\rho U}{\mu} \tag{4}$$

which is recognized as a Reynolds number. Eq. 4 can be rewritten as

$$\alpha = C\Phi Re_I;$$

where

$$\Phi = \frac{D_I - D_M}{D_I}\frac{B}{LD_I},$$

and

$$Re_I = \frac{ND_I^2\rho}{\mu} \tag{5}$$

where Φ is a function of the stirrer geometry alone. As Re_I approaches zero, α approaches zero, and the monolith must behave as an impermeable blade. For slow rotation speeds (= small α), α can be expected to be linearly proportional to Re_I. When α becomes large the pressure buildup is not as large and Eq. 4 must be modified as shown later.

The flow rate through the monolith blade can be estimated from Eq. 3 once the pressure difference is known. This is estimated from the measured torque, after subtracting the contribution from parts of the stirrer not associated with flow through the monolith, which is approximated by the measured torque of the empty tube

$$\Delta P = \frac{M_{\text{open}} - M_{\text{tube}}}{(D_I - D_M)\frac{\pi}{4}D_M^2} \tag{6}$$

The fraction of the liquid swept that passes through the blade is approximately

$$\alpha = \frac{\left(\frac{B}{L}\frac{\Delta P}{\mu}\right)}{\pi(D_I - D_M)N} \tag{7}$$

Mass transfer

Cybulski and Moulijn (1994) listed a number of correlations developed for the mass transfer from the gas phase to the wall in a narrow channel. Most of them can be written in the general form

$$Sh = Sh_\infty\left(A + BReSc\frac{d_h}{L}\right)^C \tag{8}$$

with the coefficients given in Table 1.

The overall rate of reaction in a monolith depends on both the intrinsic rate of reaction and the external mass-transfer rate. For a first-order reaction, the conversion per pass is

$$x = 1 - e^{-\frac{k_s k_r}{k_s + k_r}a_s\tau} \tag{9}$$

and for the reactor content this translates into

$$\frac{c}{c_0} = e^{-\frac{V_M}{V_L}\frac{x}{\tau}t} \tag{10}$$

Results

Hydrodynamics

Figure 3 shows measured torque as a function of stirrer speed for monoliths of two diameters (5 cm and 8 cm) at two temperatures (approximately 20° and 55°C), since the latter provided a convenient way of varying the viscosity (1 mPa·s at 20°C and 0.5 mPa·s at 55°C). The temperature varied a few degrees between measurements within a series and the fitted parabolas are only included for illustrative purposes. Temperature corrections were used in the calculations. The

Table 1. Parameters for the Sherwood Number Correlation (Eq. 8)

Sh_∞	A	B	C	Reference
2.977	1	0.095	0.45	Hawthorn (1974)
0.0767	1	1	0.829	Bennet et al. (1991)
0.766	0	1	0.483	Ullah et al. (1992)

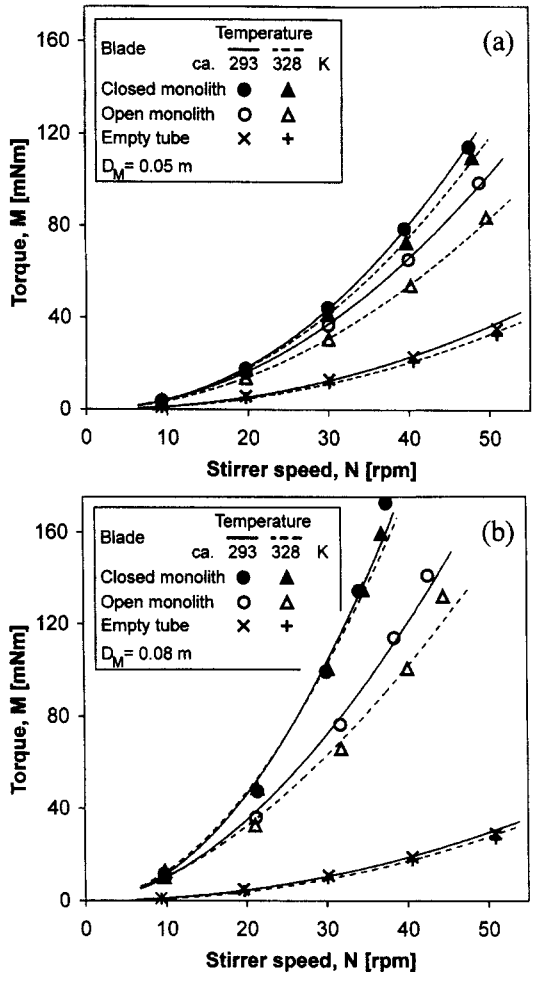

Figure 3. Measured torque vs. stirrer speed for open monolith, closed monolith, and empty tube.

a) $D_M = 0.05$ m, b) $DM = 0.08$ m.

torque of the open monolith lies in between that of the closed monolith and empty tube, proving that liquid flows through the blade. Compared to the empty tube a pressure difference is built up that drives the flow. Compared to the closed monolith there must be a flow through the monolith reducing the overall resistance of the stirrer. Temperature primarily affects the viscosity, which can be seen most clearly in Figure 3b: the open monolith exhibits a clear viscosity dependency, while this is not the case for the closed monolith.

Figure 4 shows the corresponding power numbers (the temperature variation between individual measurements is taken into account) with lines added for illustration. First consider the 5 cm monolith. For the closed monolith we find a nearly constant power number indicating that inertial forces dominate. For the open monolith the power number decreases with RE_l, which can be explained by the frictional contribution from the channel flow. Moreover, in the limit $Re_l = 0$ there is no flow through the blade and the power number should be the same in both cases, which is apparent from Figure 4. The situation is more complicated for the larger 8 cm monolith, most likely due to wall effects. First, if we take into account that the closed monoliths correspond to

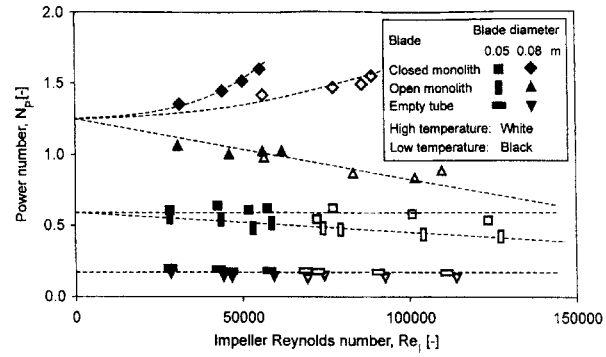

Figure 4. Power number vs. impeller for open monolith, closed monolith, and empty tube.

two series (high and low temperature), we obtain the same value in the limit of $Re_l = 0$ (see dashed lines in Figure 4). The wall, and to a larger extent the baffles, limit the free space surrounding the blade through which deflected liquid must pass. This effect is much more pronounced for the large blade since there is more liquid to deflect and less space available. Wall effects do complicate the description of the phenomena, but are desirable since they promote flow through the catalyst blade.

The resulting linear velocities are shown in Figure 5. In accordance with the previous discussion, we see that flow through the monolith blade is promoted by higher temperature (i.e., larger ρ/μ ratio) and larger diameter (wall effects). It should be noted that the linear velocities through the monolith channels are much higher than those typical of packed bed reactors, even at moderate stirrer speeds.

The resulting α is shown vs. Re_l in Figure 6. For small values of α we expect a linear relationship between α and Re_l in accordance with the discussion that led to Eq. 5. By necessity this expression cannot hold for high α and Re_l. Physically, as α becomes large, less liquid is deflected around the blade and buildup of dynamic pressure is less than predicted by the model. Also, as the stirrer speed is high, a swirl

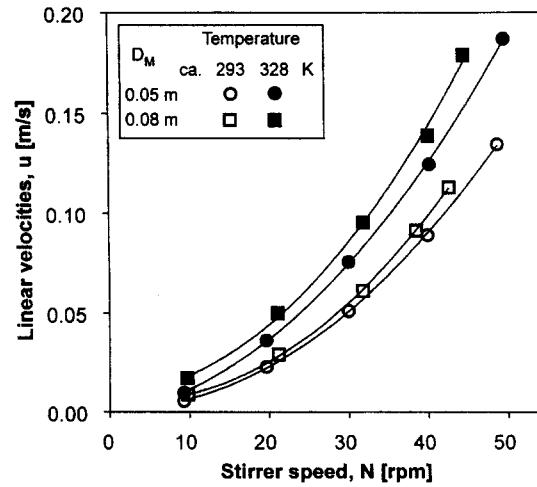

Figure 5. Linear velocities in monolith channels as a function of stirrer speed.

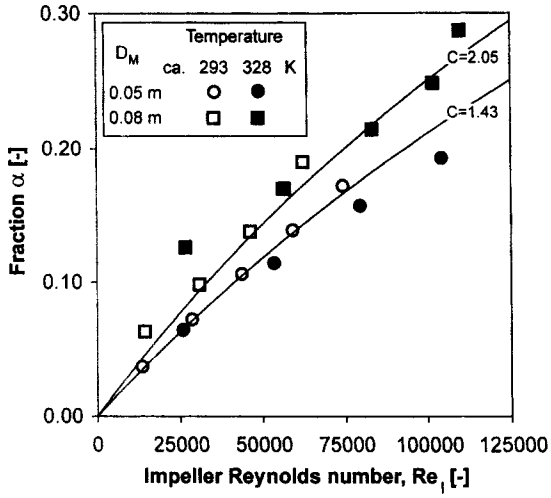

Figure 6. Fraction of liquid that passes through the monolith blade, α, as a function of impeller Reynolds number.

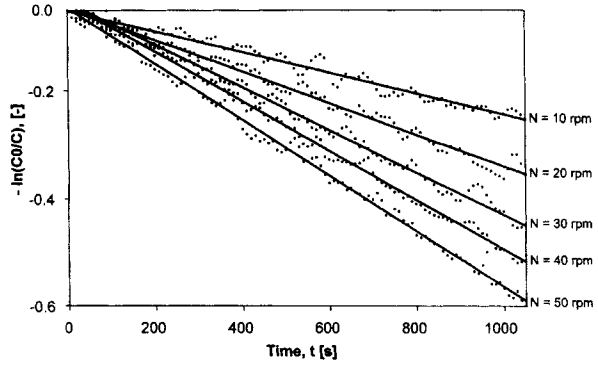

Figure 7. Decomposition rate of hydrogen peroxide as a function of stirrer speed.

For a 0.05-m diameter monolith catalyst blade.

is induced and the relative velocity between the blade and the surrounding liquid is reduced. In Figure 6 we can see that a straight line through the origin will not provide a good fit. Therefore, we suggest that the expression for the pressure difference buildup across the blade is modified by multiplying it with $(1-\alpha)$, that is, the fraction deflected by the blade. The expression for α then becomes

$$\alpha = \frac{C\Phi Re_I}{1 + C\Phi Re_I} \tag{11}$$

A least-squares fit gave $C = 1.43$ for $D_M = 0.05$ m and $C = 2.05$ for $D_M = 0.08$ m. The corresponding curves are also shown in Figure 6. The lower value appears to be appropriate when wall effects are small, while it will give a conservative estimate when wall effects are significant. The change in geometry is drastic while the change in C is moderate.

Intrinsic kinetics

The preexponential factor and the activation energy were estimated in a set of experiments carried out in a closed loop setup initially containing a 1,500-ppm hydrogen peroxide solution. The solution was pumped at high velocity (up to 1.5 L/min) through a small monolith catalyst (diameter 0.01 m and length 0.09 m) and the decrease of concentration was monitored continuously. The temperature was varied in the range 22–27°C, which gave $k_0 = 2.6 \cdot 10^4$ m/s and $E_a = 50.7$ kJ/mol. Obviously, the temperature interval is too narrow to allow an accurate estimate of the activation energy. However, the value does agree well with that reported by Ahuja et al. (1985) ($E_a = 54.5$ kJ/mol) and can be used with confidence to account for the temperature dependency within the narrow temperature range of the present study.

Mass transfer

With both mass transfer and reaction being first-order processes, we expect to find an overall first-order behavior according to Eq. 10. This is supported by Figure 7, which shows the decrease of hydrogen peroxide concentration in time for five different stirrer speeds. From the dependency on stirrer speed, it is clear that mass-transfer resistance plays an important role.

Knowing the reaction rate constant allows the estimation of the external mass-transfer coefficient. We can estimate the linear velocity through the monolith on the basis of the measured torque as shown previously. Combining this with the correlations taken from the literature provides a second estimate of the mass-transfer coefficient. These two types of estimates are shown in Figure 8. The agreement is good, in particular with the correlation of Bennet et al. (1991). Moreover, since the limiting Sh number for an infinitely long square channel is 3.0 we can conclude that we are operating completely in the region of mass transfer, which is dominated by entrance effects. For gas-phase processes this is typically not the case because of the much higher diffusivities of gaseous species, and hence shorter entrance lengths. Entrance length for concentration is approximately 0.05 $Re\ Sc\ d_h$, and Sc is in the order of 1 for gases and in the order of 1,000 for liquids.

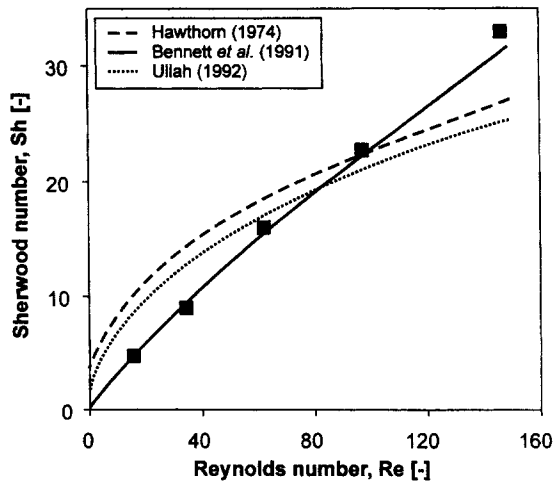

Figure 8. Sherwood numbers.

Measured and predicted based on torque measurements and correlation with literature.

Conclusions and Future Work

The present investigation clearly shows that a monolithic catalyst stirrer is a working reactor concept. By using a highly permeable monolithic blade, it becomes possible to create a large geometrical surface area and still maintain sufficient flow through it. The purpose of the present design was to study the basic hydrodynamic behavior and obtain the governing equations.

However, the design has not been optimized yet. The results of this study suggest that there is much to gain from optimization. The effects of baffles and the vessel wall are here favorable since they promote flow through the structure. Computational fluid dynamics could be a valuable tool for improving the understanding of the flow patterns in the vessel and to guide us to better designs. Also, the very high flow rates through the blades suggest that larger and/or additional blades could be used, in order to further increase the area of catalyst available for reaction.

An interesting aspect not covered here is the mixing. Compared to a conventional impeller which generates a small mixing zone of high intensity, the monolith blade generates a much larger mixing zone of low intensity. As a liquid passes through a channel it is stretched and is folded between passages. Preliminary calculations indicate that the combined mixing from a large number of channels can be very effective, and this deserves to be studied further.

The monolithic catalyst stirrer reactor can be viewed as an immobilized-slurry reactor. The short internal diffusion distances and the large external surface area are retained, but many of the problems of handling a suspension if the catalyst is finely divided are eliminated. It is a general concept which can be particularly useful in the fine chemicals sector and the biotechnology industry.

Notation

A = constant in Eq. 8
A_{open} = open frontal area
a_s = geometrical surface area of monolith, m^2/m^3
B = permeability coefficient of monolith, m^2
B = constant in Eq. 8
c = concentration of hydrogen peroxide, mol/m^3
C = constant in Eqs. 5, 8 and 11
d_h = hydraulic channel diameter (= side length), m
D_M = diameter of monolith blade, m
D_I = stirrer diameter, m
D = molecular diffusivity, m^2/s
E_a = activation energy, J/mol
k_r = rate constant, m/s
k_0 = preexponential factor, m/s
k_s = mass-transfer coefficient, m/s
L = length of monolith channel, m
M = torque on stirrer shaft, N·m
N = stirrer speed, L/s
P = stirrer power, W
P = pressure, Pa
r = rate of hydrogen peroxide decomposition, $mol/m^2 \cdot s$
R = gas law constant, J/mol·K
Sh_∞ = parameter in Eq. 8
T = temperature, K
u = linear velocity in monolith channel, m/s
u_{sup} = superficial velocity through monolith blade, m/s
V_L = total liquid volume, m^3
V_M = total monolith volume, m^3

Dimensionless numbers

N_p = power number, $P/(N^3 D_I^5 \rho)$
Sc = Schmidt number, $\mu/(D\rho)$
Sh = Sherwood number, $k_s d_h/D$

Greek letters

μ = viscosity, Pa·s
ρ = density, kg/m^3
τ = residence time in monolith channel, s

Literature Cited

Ahuja, L. D., D. Jareshwer, and K. C. Nagpal, "Decomposition of Hydrogen Peroxide on Manganese Oxide Surfaces," *Adv. in Catal. Sci. & Tech.*, Prasada Rao, ed., Wiley, New Delhi, 563 (1985).

Bennett, C. J., S. T. Kolaczkowksi, and W. J. Thomas, "Determination of Heterogeneous Reaction Kinetics and Reaction Rates under Mass Transfer Controlled Conditions for a Monolithic Reactor," *Trans. Inst. Chem. Eng.*, **69**, 209 (1991).

Carberry, J. J., "Designing Laboratory Catalytic Reactors," *Ind. Eng. Chem.*, **56**, 39 (1964).

Coulson, J. M., and J. F. Richardson, *Chemical Engineering*, Vol. 2, Pergamon, Oxford (1985).

Cybulski, A., and J. A. Moulijn, "Monoliths in Heterogeneous Catalysis," *Catal. Rev.-Sci. Eng.*, **36**, 179 (1994).

Hawthorn, R. D., "Afterburner Catalysis—Effects of Heat and Mass Transfer Between Gas and Catalyst Surface," *AIChE Symp. Ser.*, **70**, 428 (1974).

Houterman, M. J. J., *Monolithic Catalyst Stirrer Reactor*, Graduation Report, Delft Univ. of Technology, The Netherlands (1997).

Kapteijn, F., A. D. van Langeveld, J. A. Moulijn, A. Andreïni, M. A. Vuurman, A. M. Turek, J.-M. Jehng, and I. E. Wachs, "Alumina-Supported Manganese Oxide Catalysts," *J. Catal.*, **150**, 94 (1994).

Kolaczkowski, S. T., and S. Serbetcioglu, "Preparation of Siloxanes Using Heterogeneous Catalyst on Monolithic Support," EP 605143 A2 (1995).

Perry, R. H., and D. W. Green, *Perry's Chemical Engineers' Handbook*, McGraw-Hill, New York (1984).

Shah, R. K., and A. L. London, "Laminar Flow Forced Convection Heat Transfer and Flow Friction in Straight and Curved Ducts—A Summary of Analytical Solutions," Tech. Rep. No. 75, Stanford Univ., Palo Alto, CA (1971).

Turek, F., and H. Winter, "Effectiveness Factor in a Three-Phase Spinning Basket Reactor: Hydrogenation of Butynediol," *Ind. Eng. Chem. Res.*, **29**, 1546 (1990).

Ullah, U., S. P. Waldram, C. J. Bennet, and T. Truex, "Monolithic Reactors: Mass Transfer Measurements under Reacting Conditions," *Chem. Eng. Sci.*, **47**, 2413 (1992).

Vergunst, T., E. Grolman, R. K. Edvinsson, F. Kapteijn, and J. A. Moulijn, "Liquid-to-Solid Mass Transfer in Single- and Two-Phase Flow Through a Monolithic Catalyst Reactor," *Int. Conf. on Gas-Liquid-Solid Reactor Eng.*, Kanagawa, Japan (1997).

Wilke, C. R., and P. Chang, "Correlation of Diffusion Coefficients in Dilute Solutions," *AIChE J.*, **1**, 264 (1955).

Wu, Y., M. H. Al-Dahhan, M. R. Khadilkar, and M. P. Dudokovic, "Evaluation of Trickle Bed Reactor Models for a Liquid Limited Reaction," *Chem. Eng. Sci.*, **51**, 2721 (1996).

Manuscript received Nov. 19, 1997, and revision received Aug. 3, 1998.